Enhanced Methodology to Characterize 3-D Power Monitoring and Control Features for 5G NR Systems Embedding Multi-User MIMO Antennas

Sara Adda, Tommaso Aureli, Stefano D'Elia, Daniele Franci, Nicola Pasquino, *Senior Member, IEEE*, Settimio Pavoncello, and Riccardo Suman

***Abstract*— Multi-User MIMO (MU-MIMO) is widely used in the fifth generation (5G) cellular network to improve network performance at high traffic loads. When demonstrating the compliance of 5G antennas with the radio frequency (RF) electromagnetic fields standards, beamforming and MU-MIMO must be considered, since a 5G MU-MIMO antenna radiation pattern changes in both the space and time domain, adapting to changes of the user's position. To cope with the time and space variability of the power radiated by 5G systems, mobile operators can activate automatic tools to monitor and control the transmitted power (power lock (PL) systems) to ensure that a given radiated power threshold is not exceeded. This article extends and enhances the methodology introduced by the authors in previous work, by testing and verifying PL systems in an MU-MIMO and beamforming scenario (3-D PL systems, 3DPL) through field measurements, controlling the power transmitted by each beam, i.e., in each direction. Measurement results confirm that the 3DPL feature limits the average power of the traffic channels transmitted in each direction, regardless of the configured total maximum power. More specifically, it is shown that the 3DPL reduces the maximum average transmitted power by the expected 2 dB when only one user is active (i.e., in a single-user MIMO (SU-MIMO) scenario), while it does not operate any reduction when two users are active (MU-MIMO scenario) because the power transmitted toward each user is already half (i.e., −3 dB) of the maximum power that can be transmitted.**

***Index Terms*— Electromagnetic fields, exposure assessment, fifth generation (5G), human exposure, measurements, Multiple-Input Multiple-Output (MIMO), Multi-User MIMO (MU-MIMO), new radio, power lock (PL), power monitoring and control.**

I. Introduction

EXPOSURE to radio frequency (RF) electromagnetic fields is regulated worldwide by standards [1] or guidelines [2], [3] that specify limits in terms of time-averaged quantities. In Europe, which falls under the International Commission on Non-Ionizing Radiation Protection (ICNIRP) [4] guidelines, the time average had to be run for 6 min [2] until the revised version [3] extended it to 30 min. Every source of RF electromagnetic radiation is, therefore, surrounded by an *exclusion zone* that is a volume around the source where exposure is not compliant with limits and where, as a consequence, no human being should be allowed to avoid hazards related to health effects of radiations.

The fifth generation (5G) radio interface represents a major step forward in radio technology compared to previous generations and a challenge related to measurement, testing, and validation of 5G performance [5]. Indeed, 5G was designed to cover multiple usage scenarios, from mobile broadband to ultra-reliable low latency communications (URLLC) and machine-to-machine (M2M) communications. The radio interface, therefore, had to be defined to cover many different application scenarios. From a technical point of view, this required the exploitation of new technological paradigms [6]: 5G makes use of a high degree of flexibility, both in the code domain (e.g., flexible numerology), in the time domain (e.g., time-domain duplex (TDD) pattern variability), and in the frequency domain (e.g., it does not require a specific bandwidth), as well as in the space domain: this last aspect was the most relevant from the point of view of the standardization of calculation and measurement of the electromagnetic field, which for the first time had to deal with a technology—the so-called massive MIMO (MaMIMO) technology—that allows the beam to be directed, through a technique named *beamforming*, specifically toward the user in order to optimize the use of the time and space resources of the communication channel, also avoiding signal transmission where it is not needed. The complexity of the configuration of the time and space pattern of the field radiated by 5G antennas, which guarantees an unprecedented level of efficiency in the use of radio resources in space and time, required an update of the techniques for measuring and estimating the level of the electromagnetic field generated by a 5G radio base station.

When determining the exclusion zones of RF electromagnetic fields for MaMIMO antennas installations, it is important to consider the beamforming and Multi-User MIMO (MU-MIMO) [6], [7], [8] functionality of the antenna systems, that modify the radiation pattern in both the space and time

Manuscript received 24 March 2023; accepted 27 May 2023. Date of publication 8 June 2023; date of current version 22 June 2023. The Associate Editor coordinating the review process was Dr. Kamel Haddadi. *(Corresponding author: Nicola Pasquino.)*

Sara Adda is with the Agenzia Regionale Protezione Ambiente Piemonte (ARPA Piemonte), Ivrea, 10015 Turin, Italy (e-mail: sara.adda@arpa.piemonte.it).

Tommaso Aureli, Daniele Franci, and Settimio Pavoncello are with the Agenzia Regionale Protezione Ambiente Lazio (ARPA Lazio), 00187 Rome, Italy (e-mail: tommaso.aureli@arpalazio.it; daniele.franci@arpalazio.it; settimio.pavoncello@arpalazio.it).

Stefano D'Elia and Riccardo Suman are with Vodafone Networks, Mobile Access Engineering, Ivrea, 10015 Turin, Italy (e-mail: stefano.delia@vodafone.com; riccardo.suman@vodafone.com).

Nicola Pasquino is with the Dipartimento di Ingegneria Elettrica e delle Tecnologie dell'Informazione, Università degli Studi di Napoli Federico II, 80125 Naples, Italy (e-mail: nicola.pasquino@unina.it).

Digital Object Identifier 10.1109/TIM.2023.3284016

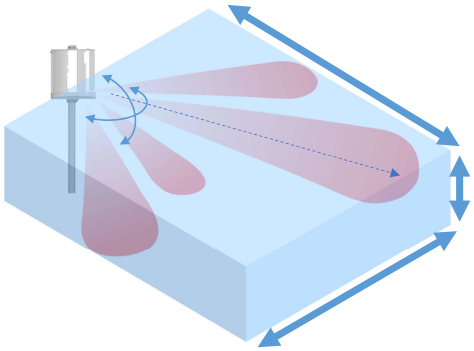

Fig. 1. Envelope diagram.

domain to adapt the electromagnetic footprint to changes of the user's position. With standard IEC 62232 [9] and the associated technical report TR 62669 [10], the International Electrotechnical Committee (IEC) identified the *envelope diagram* (see Fig. 1) as a means to evaluate the worst case radiation pattern generated by MaMIMO antennas.

The envelope diagram is obtained by considering, for each direction, the highest gain of all the beams that the antenna can synthesize in that direction. It follows that:

1) the horizontal compliance distance depends on the maximum gain of a single beam and
2) the vertical and transverse compliance distances depend on the maximum angles at which the antenna can direct the beams.

As mentioned above, it should be remembered that exposure limits are always intended as the average over a given time interval. The envelope diagram is, therefore, a purely theoretical representation, far from reality because it does not take into account either the power split among the currently active beams or the space diversity typical of MaMIMO antenna, which focuses the signal only on some sub-areas/regions of the coverage area. This means that the calculation of the electromagnetic field (EMF) exclusion zones through traditionally used methods generates very conservative results because they assume that the maximum power is transmitted simultaneously in every possible direction, due to the use of the envelope diagram, and that the MaMIMO antenna's downlink frame is full.

To consider both the time and space variability of power radiated by an MaMIMO system [11], the IEC, therefore, associates the definition of the actual maximum transmitted power (AMTP) [12], [13], [14] to the envelope diagram. AMTP is based on the space and time distribution of the transmitted power, and its numerical definition involves using, in the EMF exclusion zones of an MaMIMO antenna, the 95th percentile of the empirical distribution obtained from historical data of the power radiated by the antenna, instead of the maximum configured one.

Alternatively, the IEC [9] suggests that operators activate automatic tools to monitor and control the transmitted power of MaMIMO system—named power lock (PL) systems in the following, for short—to ensure that the threshold values configured for each antenna are not exceeded. As soon as the function detects that the average power transmitted approaches the threshold defined by the operator, the PL will automatically reduce the power. The functionality of the PL feature, which allows avoiding even those very unlikely cases in which the power transmitted by a beam pointing a certain direction is higher than the AMTP, can be tested on-site, and the IEC itself immediately took to define an adequate test procedure (see *Annex C—Guidelines for the validation of power or EIRP control features and monitoring counter(s) related to the actual maximum approach* in [9]). It must be pointed out that all the methodologies available in the literature have been validated with Single-User MIMO (SU-MIMO) antennas only and time-averaged transmitted power, therefore, without considering the MU-MIMO mode and spatial multiplexing of the beamforming antenna.

Since RF EMF exclusion zones can cause implementation problems for the operator, operators can benefit from using a more realistic exclusion zone calculation based not only on time-averaged transmitted power but also considering beamforming and the MU-MIMO functionality, while continuing to comply with exposure limitations.

The approach proposed in this article enhances and completes the methodology first introduced by Adda et al. [15] and presented also in [12], and the normative documents for characterizing and testing the PL in an MU-MIMO and beamforming scenario, controlling the power transmitted by each beam, i.e., in each direction. Such functionality will be referred to as 3-D PL (3DPL). The main novelty of the proposed approach is that the procedure in [15] only focused on PL features that operate according to the total power radiated by the antenna, while the new procedure also considers how that power is used, i.e., whether it is directed toward a single user or to multiple users, and operates accordingly.

The research presented in the article is complementary to other works spanning the 5G measurement world. Betta et al. [16] present general issues and research topics related to the measurement of human exposure to cellular networks, while [17], [18], [19], [20], [21], and [22] present the results and discussions more specific to 5G measurements methodologies and the results of experimental campaigns in urban scenarios. Furthermore, some of the authors have recently published the results of an extended experimental campaign about the impact of 5G signals on the response of wideband electric filed probes [23]; while in [24], a methodology to assess human exposure based on scalar and vector measurements of the traffic signals is proposed, following the results of [25].

The article is organized as follows. In Section II, the operating principle of the MU-MIMO smart antenna and the 3DPL is presented, while in Section III, the methodology to characterize the 3DPL in an MU-MIMO environment is described and validated, and the results are compared with the PL characterization presented in [15] in an SU-MIMO scenario. Section IV eventually summarizes the main results.

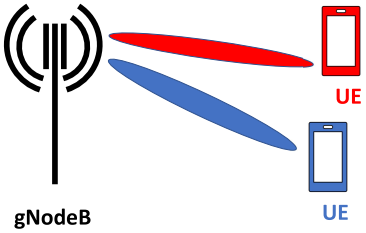

Fig. 2. MaMIMO directive beams.

II. MU-MIMO AND 3DPL

MaMIMO antennas are one of the technologies that mostly contribute to the outstanding performance of 5G NR systems [8]. They can adapt their radiation pattern dynamically with the transmission needs determined by the user's configuration within the service area. MaMIMO antennas are made of many elementary micro-antennas or arrays of antennas (for example, with 32 or 64 elements)—hence the adjective *Massive*—which work in a coherent and orchestrated way to dynamically create extremely directional radiation lobes using sophisticated signal processing techniques. The more the antennas are used, the narrower the beam can be so that lobes are more directive than those of traditional antennas and can be directed toward the position of a single user equipment (UE) (see Fig. 2). To track moving users and limit the interference in areas where the signal is not needed—and, therefore, no power is required in that direction—radiation directions change frequently, the time rate being typically equal to the transmission time interval (TTI) (that is, hundreds of milliseconds) or, at most, a few milliseconds.

The are three different array technologies that MaMIMO can use to improve both network coverage and capacity: *beamforming*, *zero-forcing beamforming*, and *spatial multiplexing* [8], [26].

The purpose of beamforming is to focus signals more in some directions than others, allowing the same frequency to be reused to carry different information over different paths to users that are spatially separated. The aim is to increase the spectral efficiency, thus improving the quality of the link in terms of signal-to-interference-plus-noise ratio (SINR), in the direction of the user of interest, due to a high beamforming gain. This results in improved network coverage and capacity, and higher performance for the user. This behavior, additionally, reduces the electromagnetic field transmitted in the cell, because the signal is sent only toward active UEs (those that are generating traffic at a specific time) and no energy is radiated toward areas where it is not necessary, that is where there are no active UEs.

In the presence of multiple active users, to obtain higher SINR and spectral efficiency for each user, the *zero-forcing beamforming* [8], [27], [28] is commonly used. By forcing nulls in the radiation pattern, such kind of beamforming technique tries to reduce the gain of the beam that serves each UE at angles pointing to other active UEs.

Spatial multiplexing is a multiple input multiple output (MIMO) multiplexing technique that allows the transmission of multiple data streams to the same UE or different UEs on the same temporal frequency symbol [named physical resource block (PRB)] [29]. When multiple data streams are directed to the same user, they are referred to as Single-User MIMO (SU-MIMO), while Multi-User MIMO (MU-MIMO) is the case that involves the spatial multiplexing of multiple users. Currently, MU-MIMO supports a maximum of 16 layers per cell and up to four SU-MIMO layers per user. Therefore, it is possible to have four MU-MIMO users with four layers each at the same time. If more than four MU-MIMO users are to be activated at the same time, these will have fewer assigned layers (for example, eight users with two layers each), the upper bound being 16 users with only one layer each. Examples of SU-MIMO and MU-MIMO configurations are shown in Fig. 3.

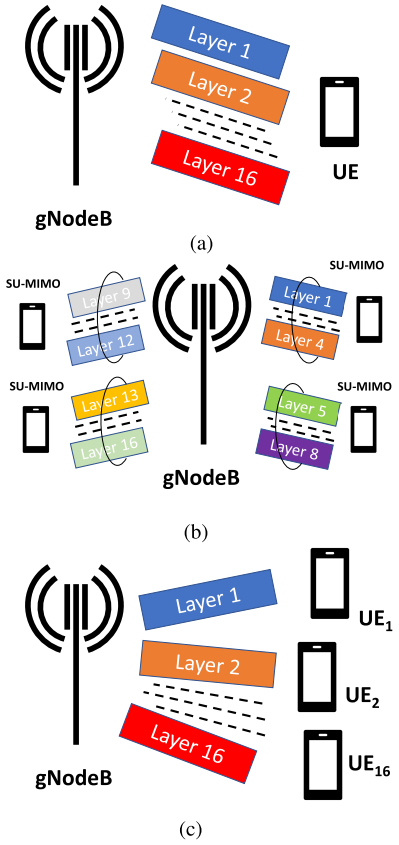

Fig. 3. Spatial multiplexing: SU-MIMO versus MU-MIMO. (a) SU-MIMO. (b) MU-MIMO (4 UEs). (c) MU-MIMO (16 UEs).

The key distinction between SU-MIMO and MU-MIMO comes down to the number of users it can assign its spectrum at the same time. In an SU-MIMO system, for instance, one portion of the spectrum (the PRB) is assigned to a single user. The SU-MIMO is the same MIMO we know from LTE networks designed to work with "traditional" antennas where the signal is transmitted over the whole service area: the direction in which the radiated energy is transmitted is fixed and determined over time. MU-MIMO expands and fuses the concepts of beamforming and spatial multiplexing, allowing the reuse of PRBs among many users, assuring low interference among them.

To show how this can be achieved, we can resort to the example of a user with an average download speed of 1 Gb/s in an SU-MIMO scenario using all PRBs available in the 5G

bands [6]. If four other users connect to the same cell, the initial speed will decrease because bandwidth and PRBs are finite and must be shared among five users instead of only one. For all five UEs to experience the same speed as one (i.e., 1 Gb/s), 5× more PRBs would be needed on average. This can be obtained with the MU-MIMO since the same PRBs can be shared among multiple users.

A challenge to be addressed by MU-MIMO is that the total instantaneous transmitted power (P_t) is split among multiple users: the maximum instantaneous transmitted power ($P_{t,\max}$) can not be higher than the maximum power configured at the antenna input ($P_{\max}$). Therefore, as the number of connected UEs increases, the power assigned to each one is reduced and, consequently, a reduction of the SINR occurs. The rules and strategies to split the power among MU-MIMO users are completely up to the manufacturer (and, as such, patented), but more information on this is available in [7].

To better understand the differences between the PL and the 3DPL features, we can go back to the example mentioned above. For the sake of ease, we will assume that the system has an technology duty cycle factor (F_{TDC}) [9] equal to 1, i.e., that the TDD is used 100% of the time for the downlink. If the PL is configured so that the threshold for the average power over 6 min $P_{\text{avg,max}}$ is at 25% $P_{\max}$, in the SU-MIMO scenario, with a single user requiring full resources (i.e., 100% PRBs), the antenna constantly transmits in a specific direction at $P_{\max}$. This condition will activate the PL, which will reduce P_t, so that the average power over the entire 6-min interval will be 25% $P_{\max}$.

If four more users, spatially separated, connect to the same cell, and all of them require full resources (i.e., 100% PRBs), due to the MU-MIMO, the same PRBs can be shared among multiple users and they can experience the same speed as the first one. The antenna is now constantly transmitting in five different directions, the total power being homogeneously divided among all users so that each user is reserved 20% $P_{\max}$. However, since the PL monitors the total power transmitted by the antenna, the feature reduces P_t so that the total average power of the five connections over the 6-min integration interval is 25% $P_{\max}$, with an impact on the signal-to-noise ratio (SNR) and the overall performance of the system: when PL is active, the transmitted power reserved for each user is 20% $P_{\text{avg,max}}$, i.e., only 5% $P_{\max}$. Instead, if we adopt a per-beam reduction strategy, which is what a 3DPL does, the system detects that, in each of the five directions, the transmitted power (20% $P_{\max}$) is lower than the threshold $P_{\text{avg,max}}$ and will not activate.

The purpose of MU-MIMO is to improve network performance at high traffic loads under good SINR conditions. These are conflicting requirements, as high traffic loads often result in lower SINR due to increased network interference. The PL would worsen the channel conditions by excessively limiting the power in high-traffic load conditions, while the 3DPL allows a better SINR than the PL. The primary benefit of using MU-MIMO and 3DPL jointly is that they improve performance at high traffic loads and allow the reuse of spectrum and infrastructure to serve multiple users, without any significant performance degradation while continuing to comply with exposure regulations strictly. The 3DPL monitors the power transmitted by the MaMIMO system in the space and automatically limits the maximum value only for the beam pointing in a specific direction where the average power over a reference time interval is about to exceed the allowed threshold.

TABLE I
SPECTRUM ANALYZER CONFIGURATION

Parameter	Value
Reference Level	0 dBm
Attenuation	10 dB
Resolution bandwidth (RBW)	100 kHz
Video bandwidth (VBW)	300 kHz
Center Frequency	3.68 GHz
Frequency Span	163 MHz
Integration band	80 MHz
Trigger mode	Auto sweep
Trace mode	Average
Averaged traces	100

III. CHARACTERIZATION OF 3DPL IN MU-MIMO ENVIRONMENT

A. Measurement Setup

The capability of the 3DPL to control the power transmitted in each direction was tested in the same line-of-sight (LOS) environment used to validate the PL methodology presented in [15] (see Fig. 4). Two points on the ground, sufficiently away from each other to activate different traffic beams, were identified based on the beams' radiation pattern provided by the MaMIMO antenna manufacturer. Two 5G mobile phones (UE_1 and UE_2 in Fig. 4) were positioned at the measurement points and configured with continuous User Datagram Protocol (UDP) data transmission.

To measure the channel power (CP) at the point close to UE_1, an Rohde & Schwarz (R&S) FSVA 3030 spectrum analyzer, configured as shown in Table I and connected to a Keysight N6850A isotropic broadband antenna, was used. A power counter and a dedicated software provided by the antenna vendor were also used during the measurement session to sample both P_t and traffic [i.e., the number of transmitted resource blocks (RBs)] at the input of the MaMIMO antenna.

The measurement campaign consisted in repeating the validation procedure described in Section III-B three times. Sample statistics of the three CP measurements is reported in the two rightmost columns of Table II.

B. Experimental Results

The PL feature presented in [15] and [12] measures the maximum average power transmitted by the antenna regardless of the direction in which it is radiated. The PL does not consider the beamforming and spatial multiplexing array technologies of an MaMIMO antennas. In fact, the PL incorrectly assumes that the radiated power for each direction is equal to the total power transmitted by the antenna, which is equal

Fig. 4. Measurement site and UE position.

TABLE II
TEST CONFIGURATION AND SUMMARY OF MEASUREMENTS

Test no.	t	UE_1	UE_2	3D PL	P_t	F_{TDC}	$P_{avg,max}$ to UE_1	$P_{avg,max}$ to UE_2	$\bar{CP}$	s_{CP}
4	t_0	ON	OFF	Operating	51 dBm	−1.3 dB	49.7 dBm	0 dBm	−15.47 dBm	0.12 dB
	t_1	ON	OFF		49 dBm		47.7 dBm (= P_0)	0 dBm	−17.51 dBm	0.15 dB
5		ON	ON	Not Operating	51 dBm	−1.3 dB	46.7 dBm	46.7 dBm	−18.55 dBm	0.13 dB
6	t_2	ON	OFF	Operating	51 dBm	−1.3 dB	49.7 dBm	0 dBm	−15.58 dBm	0.13 dB
	t_3	ON	OFF		49 dBm		47.7 dBm (= P_0)	0 dBm	−17.62 dBm	0.15 dB

to the sum of the powers radiated to each user. To prove that the methodology presented in [15] can be extended to the testing of 3DPL systems, we replicated the procedure illustrated therein, yet extending some steps—as will be shown later—to consider the activation of two different beams (see the flowchart in Fig. 5). For the same reason, test numbers in each step continue the numbering of those reported in the original paper, therefore, starting at No. 4 as shown in Table II.

The reason for limiting the experimental activity to $k = 2$ UEs only is because [8], [30], and [31] show that if there are $k \geq 2$ different UEs activating k beams at maximum power, the maximum power that the system can radiate will be split homogeneously among the beams. Consequently, the power assigned to each beam will be $P_{max} - \log(k)$. Therefore, if $k = 2$ users make the average power below the maximum allowed average power P_0, more so will do $k > 2$ users.

For the experimental campaign, $F_{TDC} = -1.3$ dB and $P_{max} = 51$ dBm. Therefore, the maximum average power that can be transmitted by the MaMIMO system in a specific direction over a 6-min interval when the 3DPL is inactive and $P_t = P_{max}$ is $P_{avg,max} = P_{max} - |F_{TDC}| = 49.7$ dBm. The 3DPL's threshold for the maximum total average power over 6 min P_0 is 2 dB[1] below $P_{avg,max}$, i.e., $P_0 = P_{avg,max} - 2$ dB $= P_{max} - |F_{TDC}| - 2$ dB $= 47.7$ dBm.

Measurements of P_t (both in dBm units and W), RBs, and the status of the two UEs for one of the three experiments run in the campaign are shown in Fig. 6. Before test No. 4 starts, both UEs are off and the MaMIMO system is not powered.

[1]1.5-dB power drop is fixed by the service provider, 0.5-dB additional reduction is applied by the manufacturer (adding to whatever the threshold configured by the service provider).

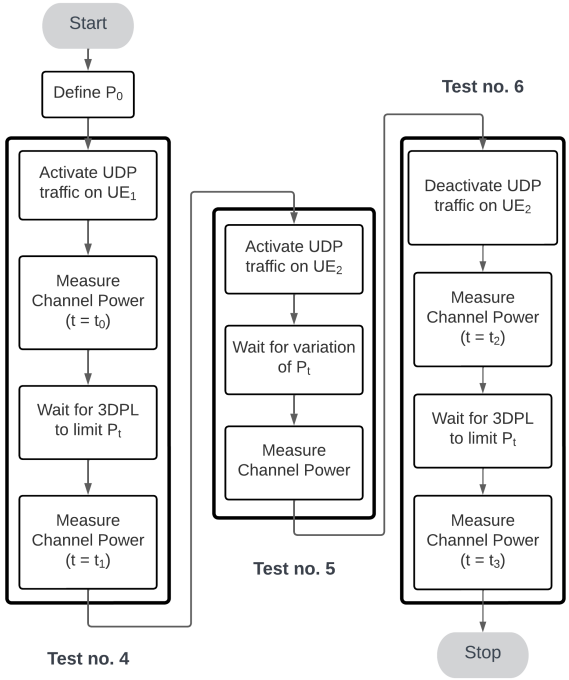

Fig. 5. Flowchart.

The flowchart in Fig. 5 shows the steps of each test described in the following.

1) Test No. 4: UE_1 ON and UE_2 OFF: The test starts when the antenna is switched on and UE_1 is activated and starts transmitting. As expected, given the UDP configuration, P_t is the maximum available power—i.e., $P_t = P_{max}$—and all RBs are transmitted (see the left frame in Fig. 6). At $t = t_0$, the

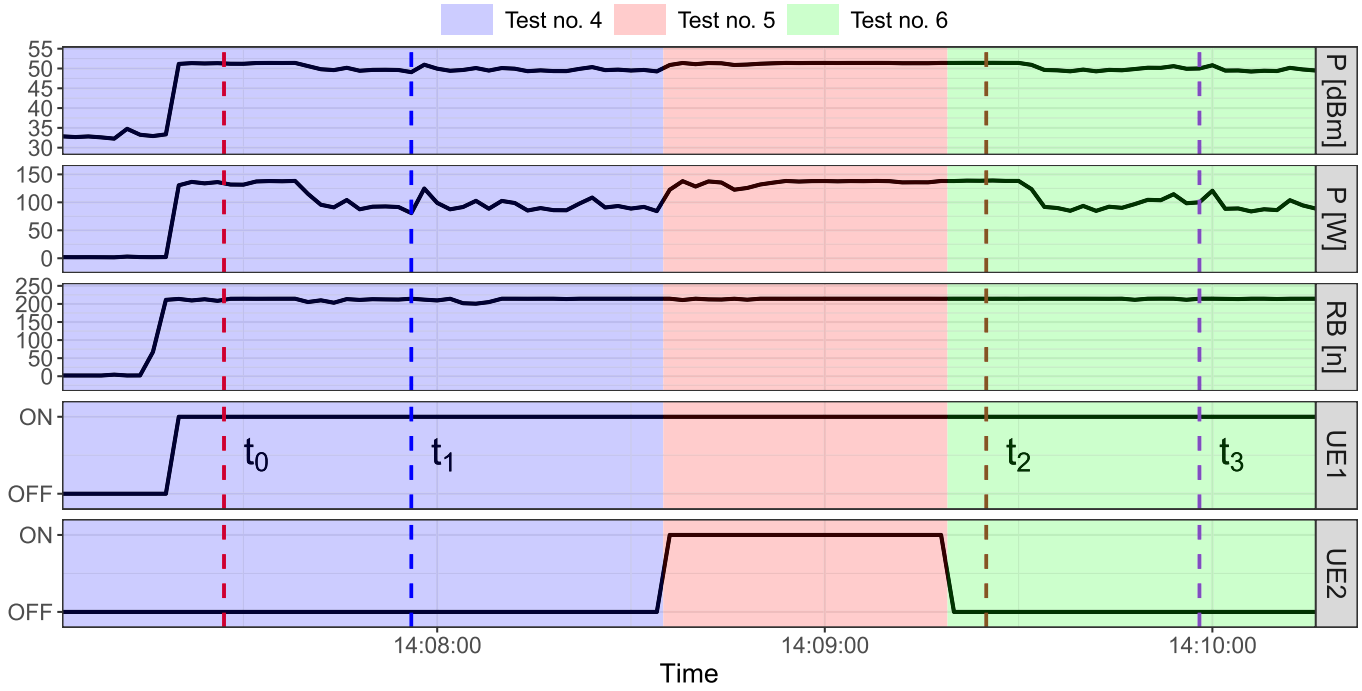

Fig. 6. Instantaneous power (P_t), transmitted RBs, and UE status.

instantaneous power is not limited by the 3DPL yet, because the current total average power P_{avg} is less than the threshold P_0. As P_{avg} increases with time, the 3DPL senses that P_0 is being approached and starts limiting the instantaneous power at $P_t = P_0$. A measurement at $t = t_1$, when limitation is active, proves that there is a reduction of the CP and, therefore, of the exposure.

The sample means of CP measurements obtained before power limitation are applied (i.e., at various $t = t_0$, when the MaMIMO transmits at $P_t = P_{max}$) and during power limitation (i.e., at various $t = t_1$, when power is limited at P_0) are -15.47 dBm ($s = 0.12$ dB) and -17.51 dBm ($s = 0.15$ dB), respectively (see Table II). This confirms that the 3DPL feature limits the average transmitted power by 2 dB, as expected. Fig. 7(a) and (b) shows that both before ($t = t_0$) and after ($t = t_1$) application of the limitation, all RBs are transmitted.

In this phase, the 3DPL operates as in Test No. 3 in [15] because there is only one active user in a single direction (it is an SU-MIMO scenario), and the power radiated toward that direction is the whole power transmitted by the antenna. There is, therefore, no difference between the 3DPL and the PL, and it is possible to monitor the transmitted power trend through P_t.

2) Test No. 5: UE_1 ON and UE_2 ON: Test No. 5 starts when UE_2 starts UDP transmission, with UE_1 still active and the 3DPL limiting power.

As expected, data keeps being transmitted with the maximum number of RBs available, and the instantaneous power measured at the antenna terminal goes back to $P_t = P_{max}$ (see the center frame in Fig. 6). This happens because the system is configured in MU-MIMO mode, and the scheduler splits the power between the two users (see Fig. 2). This implies that the maximum power that can be transmitted by the MaMIMO system in a specific direction is now $P_{max} - 3$ dB $=$ 48 dBm, since there are two active users. Therefore, now the power transmitted in each direction is less than the threshold ($P_{max} - 3$ dB $< P_0$) and the 3DPL is not required to operate any further reduction.

The sample mean of CP measurements during this test is -18.55 dBm ($s = 0.13$ dB) (see Table II), that is, 3.08 dB below the mean value obtained without any reduction applied.

In this situation, the 3DPL does not limit P_t, because it is not monitoring and controlling the total power transmitted by the antenna, but the power transmitted in each direction. This is where the per-beam behavior of the 3DPL feature shows.

Indeed, if a PL was embedded in the antenna system, P_0 would be split between the two active users since the total average power transmitted over 6 min cannot exceed P_0, to comply with the limit. As a result, in Test No. 5, the activation of PL would result in P_0 being reduced by 3 dB compared to the single user scenario described in Test No. 4, and that would, therefore, return a CP measurement equal to -17.51 dBm $- 3$ dB $= -20.51$ dBm, i.e., the value measured at $t = t_1$ reduced by the 3 dB due to the power split. By using the 3DPL there is a net improvement of 2 dB in the CP at the user side compared to what would be received when a PL is used instead.

3) Test No. 6: UE_1 ON and UE_2 OFF: Test No. 6 starts when UDP data transmission by UE_2 is interrupted. When that happens, the whole power at the antenna input is assigned to the direction pointing to UE_1. Therefore, $P_t = P_{max}$ (see $t = t_2$ in Fig. 6). Consequently, after a few seconds under this condition, the 3DPL senses that P_0 is being approached and it limits the instantaneous power P_t at $P_t = P_0$ (see $t = t_3$ in Fig. 6). Since there is only one active user, it is possible to monitor the power trend through P_t, just like in test No. 4.

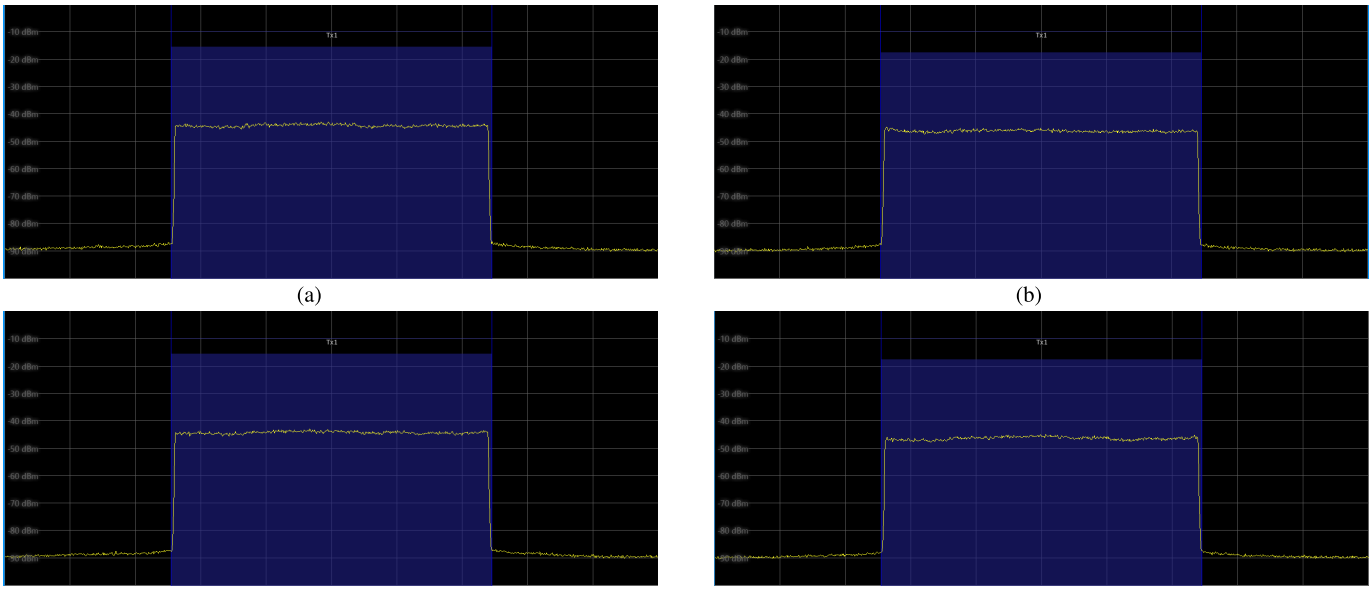

Fig. 7. CP measurements at UE_1. (a) $t = t_0$ and $P_t = P_{max}$. (b) $t = t_1$ and $P_t = P_0$. (c) $t = t_2$ and $P_t = P_{max}$. (d) $t = t_3$ and $P_t = P_0$.

This test is run to make sure that the 3DPL behaves as in test No. 4, (i.e., it reduces power to respect the maximum average power limit) even when the system exits a situation where power is limited not because of the 3DPL but because of the power split between different beams operated by the MaMIMO system itself.

The sample mean of CP measurements obtained before power limitation is applied (i.e., at various $t = t_2$, when the MaMIMO transmits at $P_t = P_{max}$) and during power limitation (i.e., at various $t = t_3$, when power is limited at P_0) are -15.58 dBm ($s = 0.13$ dB) and -17.62 dBm ($s = 0.15$ dB), respectively (see Table II). This confirms that the 3DPL feature limits the average transmitted power by 2 dB, as expected. Fig. 7(c) and (d) shows that both before ($t = t_2$) and after ($t = t_3$) activation of the limitation, all RBs are transmitted.

Results prove that, for the mobile operator, the use of 3DPL together with MU-MIMO configuration has a significant advantage. As a matter of fact, a PL worsens the channel conditions by excessively limiting the power in the case of MU-MIMO scenario, while 3DPL allows a better SINR than PL. Therefore, in the MU-MIMO scenario, the 3DPL improves performance by allowing the reuse of spectrum and infrastructure to serve multiple users, while strictly adhering to exposure standards.

IV. Conclusion

In this article, we have shown how to extend and enhance the methodology to characterize a 3DPL, an automatic tool for monitoring and controlling the average power transmitted by an MaMIMO system to make exposure to electromagnetic fields generated by 5G systems compliant with exposure limits on a per-beam basis. The proposed extension requires that the transmitted power and the resulting electromagnetic field strength are monitored under three different conditions, thus the validation procedure requires three different operations.

The experimental validation shows significantly positive advantages for the mobile operator and those who perform the verification (regulatory body). On the one hand, the results prove that for a mobile operator, the main advantage of using 3DPL over PL is the possibility to improve performance at high traffic loads allowing for spectrum and infrastructure reuse to serve more users, without any significant performance degradation while continuing to comply with exposure regulations. On the other hand, the results prove that the methodology is independent of the specific implementation of the 3DPL feature and can, therefore, always be applied without loss of generality to verify that the feature maintains the designated operating characteristics over time.

More specifically, the results confirm the effectiveness of the methodology in demonstrating that the 3DPL feature limits the average power of the traffic channels transmitted in each direction, regardless of the configured maximum power. It is shown that the 3DPL reduces the maximum average transmitted power by the expected 2 dB when only one user is active (i.e., in a SU-MIMO scenario), while it does not operate any reduction when two users are active (MU-MIMO scenario) because the power transmitted toward each user is already half (i.e., -3 dB) of the maximum power that can be transmitted.

References

[1] *IEEE Standard for Safety Levels With Respect to Human Exposure to Electric, Magnetic, and Electromagnetic Fields, 0 Hz to 300 GHz*, IEEE Standard IEEE C95.1 (Revision of IEEE Std C95.1-2005/Incorporates IEEE Standard C95.1-2019/Cor 1-2019), 2019.

[2] A. Ahlbom et al., "Guidelines for limiting exposure to time-varying electric, magnetic, and electromagnetic fields (up to 300 GHz)," *Health Phys.*, vol. 74, no. 4, pp. 494–521, 1998.

[3] International Commission on Non-Ionizing Radiation Protection, "Guidelines for limiting exposure to electromagnetic fields (100 kHz to 300 GHz)," *Health Phys.*, vol. 118, no. 5, pp. 483–524, May 2020. [Online]. Available: http://journals.lww.com/10.1097/HP.0000000000001210

[4] *ICNIRP—International Commission on Non-Ionizing Radiation Protection*. Accessed: Mar. 24, 2023. [Online]. Available: https://www.icnirp.org/

[5] E. Hossain and M. Hasan, "5G cellular: Key enabling technologies and research challenges," *IEEE Instrum. Meas. Mag.*, vol. 18, no. 3, pp. 11–21, Jun. 2015.

[6] *NR; Physical Layer Procedures for Control*, document 38.213, 3GPP, 2018. [Online]. Available: https://www.3gpp.org/DynaReport/38213.htm

[7] L. Liu, G. Miao, and J. Zhang, "Energy-efficient scheduling for downlink multi-user MIMO," in *Proc. IEEE Int. Conf. Commun. (ICC)*, Jun. 2012, p. 4394.

[8] F. W. Vook, A. Ghosh, and T. A. Thomas, "MIMO and beamforming solutions for 5G technology," in *IEEE MTT-S Int. Microw. Symp. Dig.*, Jun. 2014, pp. 1–4.

[9] *Determination of RF Field Strength, Power Density and SAR in the Vicinity of Radiocommunication Base Stations for the Purpose of Evaluating Human Exposure*, Standard 62 232, 2022.

[10] *Determination of RF Field Strength, Power Density and SAR in the Vicinity of Radiocommunication Base Stations for the Purpose of Evaluating Human Exposure*, Standard IEC-TR 62669 and IEC 62232, 2019.

[11] A. Schiavoni, S. Bastonero, R. Lanzo, and R. Scotti, "Methodology for electromagnetic field exposure assessment of 5G massive MIMO antennas accounting for spatial variability of radiated power," *IEEE Access*, vol. 10, pp. 70572–70580, 2022.

[12] C. Törnevik, T. Wigren, S. Guo, and K. Huisman, "Time averaged power control of a 4G or a 5G radio base station for RF EMF compliance," *IEEE Access*, vol. 8, pp. 211937–211950, 2020.

[13] B. Xu et al., "A summary of actual maximum approach studies on EMF compliance of 5G radio base stations," in *Proc. 16th Eur. Conf. Antennas Propag. (EuCAP)*, Mar. 2022, pp. 1–5.

[14] P. Joshi, F. Ghasemifard, D. Colombi, and C. Törnevik, "Actual output power levels of user equipment in 5G commercial networks and implications on realistic RF EMF exposure assessment," *IEEE Access*, vol. 8, pp. 204068–204075, 2020.

[15] S. Adda et al., "A methodology to characterize power control systems for limiting exposure to electromagnetic fields generated by massive MIMO antennas," *IEEE Access*, vol. 8, pp. 171956–171967, 2020. [Online]. Available: https://ieeexplore.ieee.org/document/9200351/

[16] G. Betta et al., "On the measurement of human exposure to cellular networks," *IEEE Instrum. Meas. Mag.*, vol. 23, no. 9, pp. 5–13, Dec. 2020.

[17] S. Aerts et al., "In-situ measurement methodology for the assessment of 5G NR massive MIMO base station exposure at sub-6 GHz frequencies," *IEEE Access*, vol. 7, pp. 184658–184667, 2019.

[18] S. Aerts et al., "In situ assessment of 5G NR massive MIMO base station exposure in a commercial network in Bern, Switzerland," *Appl. Sci.*, vol. 11, p. 3592, Apr. 2021.

[19] C. Bornkessel, T. Kopacz, A. Schiffarth, D. Heberling, and M. A. Hein, "Determination of instantaneous and maximal human exposure to 5G massive-MIMO base stations," in *Proc. 15th Eur. Conf. Antennas Propag. (EuCAP)*, Mar. 2021, pp. 1–5.

[20] G. Betta, D. Capriglione, G. Cerro, G. Miele, M. D. Migliore, and D. Suka, "Experimental analysis of 5G pilot signals' variability in urban scenarios," in *Proc. IEEE Int. Symp. Meas. Netw.*, Jul. 2022, pp. 1–6.

[21] G. Betta, D. Capriglione, G. Cerro, G. Miele, M. D. Migliore, and D. Suka, "5G DSS communications: Pilot signals' variability analysis from measurements on the field," in *Proc. IEEE Int. Instrum. Meas. Technol. Conf. (IMTC)*, May 2022, pp. 1–6.

[22] S. Q. Wali, A. Sali, J. K. Allami, and A. F. Osman, "RF-EMF exposure measurement for 5G over mm-wave base station with MIMO antenna," *IEEE Access*, vol. 10, pp. 9048–9058, 2022.

[23] S. Adda, L. Anglesio, F. Bogo, N. Pasquino, and S. Trinchero, "How 5G NR signals impact on the response of broadband electric field probes," *IEEE Trans. Instrum. Meas.*, vol. 72, pp. 1–8, 2023.

[24] S. Adda et al., "Methodology based on vector and scalar measurement of traffic channel power levels to assess maximum exposure to electromagnetic radiation generated by 5G NR systems," *IEEE Access*, vol. 10, pp. 12125–12136, 2022. [Online]. Available: https://ieeexplore.ieee.org/document/9690179/

[25] S. Adda et al., "A theoretical and experimental investigation on the measurement of the electromagnetic field level radiated by 5G base stations," *IEEE Access*, vol. 8, pp. 101448–101463, 2020, doi: 10.1109/access.2020.2998448.

[26] S. Suyama, J. Mashino, Y. Kishiyama, and Y. Okumura, "5G multi-antenna technology and experimental trials," in *Proc. IEEE Int. Conf. Commun. Syst. (ICCS)*, Dec. 2016, pp. 1–6.

[27] S. Lu, S. Zhao, and Q. Shi, "Block-diagonal zero-forcing beamforming for weighted sum-rate maximization in multi-user massive MIMO systems," in *Proc. IEEE Symp. Comput. Commun. (ISCC)*, Jul. 2020, pp. 1–6. [Online]. Available: https://ieeexplore.ieee.org/document/9219669/

[28] S. Fang et al., "Zero forcing assisted single layer beamforming for spatial modulation MIMO systems," *IEEE Trans. Veh. Technol.*, vol. 71, no. 4, pp. 4116–4128, Apr. 2022. [Online]. Available: https://ieeexplore.ieee.org/document/9715042/

[29] S. Chen, S. Sun, G. Xu, X. Su, and Y. Cai, "Beam-space multiplexing: Practice, theory, and trends, from 4G TD-LTE, 5G, to 6G and beyond," *IEEE Wireless Commun.*, vol. 27, no. 2, pp. 162–172, Apr. 2020. [Online]. Available: https://ieeexplore.ieee.org/document/9048614/

[30] Q. H. Spencer, C. B. Peel, A. L. Swindlehurst, and M. Haardt, "An introduction to the multi-user MIMO downlink," *IEEE Commun. Mag.*, vol. 42, no. 10, pp. 60–67, Oct. 2004.

[31] S. Ali, E. Hossain, and D. I. Kim, "Non-orthogonal multiple access (NOMA) for downlink multiuser MIMO systems: User clustering, beamforming, and power allocation," *IEEE Access*, vol. 5, pp. 565–577, 2017.

Sara Adda received the M.Sc. degree (cum laude) in physics and the master's degree in health physics from Turin University, Turin, Italy, in 1998 and 2003, respectively.

From 1998 to 1999, she was with the ENEA Casaccia Research Center, Rome, Italy, within the Interdepartmental Computing and High-Performance Networks Project, implementing a system for the simulation of electromagnetic field (EMF) dynamics in complex environments through the use of massively parallel architectures. Since 1999, she has been with the Physical and Technological Risk Department, Agenzia Regionale Protezione Ambiente Piemonte (ARPA Piedmont), Turin, Italy, dealing with control and monitoring of non-ionizing radiation and the development of theoretical forecasting/numerical calculation methods, both in the low- and high-frequency ranges. She also participates in the Italian Electrotechnical Committee (CEI) working groups, for the drafting of technical standards on measurement and evaluation methods for human EMF exposure, and deals with the theoretical and practical aspects related to the measurement of EMFs in the workplace. In this context, she is the representative of the Piedmont Region in the Interregional Technical Coordination Group. She participates in European (Twinning Italy–Poland Project) and international collaborative projects (Arpa Piemonte–Beijing Municipal Environmental Protection Bureau), on methods and techniques for measuring and evaluating human exposure to EMF both in the workplace and in the living environment.

Tommaso Aureli received the M.Sc. degree in biological science from Sapienza University, Rome, Italy, in 1985.

He joined the Agenzia Regionale Protezione Ambiente Lazio (ARPA Lazio), Rome, in 2002. From 2004 to 2018, he was the Director of the EMF Division, being involved in the measurement and provisional evaluation of electromagnetic field (EMF) from civil sources. He is currently the Director of the Department of Rome of ARPA Lazio.

Stefano D'Elia received the M.Sc. degree (magna cum laude) in electronics engineering from the University of Rome "La Sapienza," Rome, Italy, in 1997.

He joined Vodafone Italy (formerly Omnitel), Ivrea, Turin, Italy, in 1998, where he is currently covering the role of the Mobile Access Integrated Solutions Manager of Vodafone Networks. His main professional interests are energy efficiency modeling for mobile networks, and calculation and measurements for the assessment of human exposure to high-frequency electromagnetic fields from mobile base stations.

Dr. D'Elia was awarded the Vodafone Distinguished Engineer, one of the highest steps in the technical career path at Vodafone, in 2012. He has been a national delegate in several standard bodies on electromagnetic fields measurements and calculations, and since 2002, he has been the appointed Chair of the Working Group "Mobile Base Stations" within the Technical Committee 106 "Human Exposure to Electromagnetic Fields" of the Italian Electrotechnical Committee.

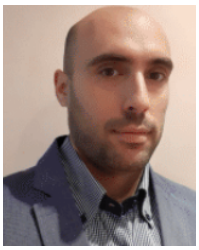

Daniele Franci received the M.Sc. (magna cum laude) and Ph.D. degrees in nuclear and subnuclear physics from Sapienza University, Rome, Italy, in 2007 and 2011, respectively.

From 2009 to 2011, he was an Analyst Technologist with Nucleco SPA, Rome, involved in the radiological characterization of radioactive wastes from the decommissioning of former Italian nuclear power plants. He joined the Agenzia Regionale Protezione Ambiente Lazio (ARPA Lazio), Rome, in 2011, being involved in RF electromagnetic field (EMF) human exposure assessment. Since 2017, he has been involved in activities of the Italian Electrotechnical Committee (CEI) for the definition of technical procedures for EMF measurement from 4G/5G multiple-input multiple-output (MIMO) sources.

Nicola Pasquino (Senior Member, IEEE) was born in Naples, Italy, in 1973. He received the M.Sc. degree (magna cum laude) in electronics engineering and the Ph.D. degree in information engineering from the Università degli Studi di Napoli Federico II, Naples, in 1998 and 2002, respectively.

He was a Fulbright Scholar with the University of Pennsylvania, Philadelphia, PA, USA, from 2000 to 2001. He is currently a Professor of electrical and electronic measurements with the Department of Electrical Engineering and Information Technologies, Università degli Studi di Napoli Federico II, where he is currently the Chief Scientist with the Electromagnetic Compatibility Laboratory, Department of Electrical Engineering and Information Technologies. His research interests include electromagnetic compatibility measurements and measurements of human exposure to high-frequency electromagnetic fields, with the application of machine learning methodologies to measurement data analysis.

Prof. Pasquino was the President of the Rotary Club Napoli Angioino (D2101, Italy), from 2019 to 2020. He has been a member of Rotary since 2005. He is the Chair of the Technical Committee 106 (TC106) "Human Exposure to Electromagnetic Fields" of the Italian Electrotechnical Committee (CEI). He is also the Chair of the Committee on "Human Exposure to Electromagnetic Fields" within the Engineering Register of Naples. He is a member of the Editorial Board of the *Measurement Science Review* journal. He serves as an Editor for the *Journal of Electrical and Computer Engineering* and a Section Editor for the *Acta IMEKO* journal.

Settimio Pavoncello was born in Rome, Italy, in 1973. He received the M.Sc. degree in telecommunication engineering from Sapienza University, Rome, in 2001.

Since 2002, he has been with the EMF Department, Regional Environmental Agency of Lazio, Rome. He is specialized in electromagnetic field (EMF) measurements and EMF projects evaluation related to radio, TV, and mobile communications systems maturing huge experience in the use of broadband and selective instruments. In the last years, he has deepened the issues related to measurements on LTE and NB-Internet of Things (IoT) signals.

Mr. Pavoncello has been actively involved in the Working Group "Mobile Base Stations" within the Technical Committee 106 of the Italian Electrotechnical Committee (CEI), since 2018, aimed at defining measurement procedures for mobile communications signals and is currently engaged in various projects concerning measurement on 5G signals.

Riccardo Suman was born in Ivrea, Turin, Italy, in 1974. He received the B.Sc. degree in telecommunication engineering from the Politecnico di Torino, Turin, in 1996.

Since 1996, he has been with Vodafone Italy (formerly Omnitel Pronto Italia), Turin, where he is currently an Antenna Matter Expert. He also participates in the BASTA (Recommendation on Base Station Antenna Standards) by NGMN Alliance. Since 2012, he has been involved in activities related to electromagnetic field (EMF) focusing on measuring and modeling electromagnetic fields and electromagnetic exposure assessment of base stations for mobile communications.

Mr. Suman also participated in the Technical Committee 106 (TC106) of the Italian Electrotechnical Committee (CEI), as a National Delegate to the International Electrotechnical Committee (IEC) TC106.

Open Access funding provided by 'Università degli Studi di Napoli "Federico II"' within the CRUI CARE Agreement